# Coupling light into organic nanofibres via Raman scattering: waveguiding properties for near-infrared light

*Ken Takazawa* ✉

*National Institute for Materials Science, 3-13, Sakura, Tsukuba 305-0003, Japan*
✉ *E-mail: takazawa.ken@nims.go.jp*

Published in Micro & Nano Letters; Received on 13th July 2016; Revised on 18th October 2016; Accepted on 31st October 2016

A technique to couple near-infrared (IR) light into organic nanofibres that function as active optical waveguides by utilising Raman scattering is developed. Using this technique, light was coupled with $\lambda = 800$–$910$ nm into an organic nanofibre of thiacyanine (TC) dye and waveguiding properties in this wavelength range were investigated. A number of organic nanofibres, including TC nanofibres, have been found to function as active waveguides that propagate their own fluorescence along themselves. The waveguiding properties of these nanofibres have been extensively investigated in their fluorescence wavelength range, which is usually in the ultraviolet to visible region. However, their waveguiding properties outside of the fluorescence range are completely unknown because of the difficulties in coupling light from an external light source. The technique enables coupling of light with various wavelengths from the visible to the near-IR into nanofibre waveguides and investigation of the waveguiding properties at these wavelengths.

**1. Introduction:** Single-crystalline micro/nanofibres that are self-assembled from some classes of organic dyes and luminescent molecules have been found to function as active waveguides that propagate the fluorescence generated by optical excitation along the fibre axis [1–4]. Owing to their nanoscale dimensions, high mechanical flexibility and low-loss waveguiding properties, including extremely small bending losses [5, 6], these nanofibre waveguides have attracted considerable attention for nanophotonics applications, such as waveguides in miniaturised photonic circuits, nanofibre lasers, and nanoscale optical devices and sensors [7–15].

Due to these nanofibre waveguides propagate their own fluorescence, waveguiding can be observed only in the wavelength range of their fluorescence band. Consequently, their waveguiding properties can be studied only in this wavelength range, which is usually from ultraviolet to visible, and those at wavelengths outside the fluorescence band are completely unknown. Therefore, one obvious question is whether these nanofibres also exhibit excellent waveguiding properties for wavelengths outside their fluorescence band. In particular, the waveguiding properties for near-infrared (IR) light are of great interest. In our previous studies, we demonstrated that photonic circuit components, such as microring resonators and Mach–Zehnder interferometers, could be fabricated on the micrometre scale using organic dye nanofibres and that they exhibited considerably high performance in the visible wavelength range [7, 8]. If these components also function in the near-IR wavelength range, they are promising for telecommunication device applications. To investigate the waveguiding properties for near-IR light, one has to couple the light into the nanofibres. However, it is technically very challenging to couple light from an external light source into nanofibres because of their nanoscale dimensions. Therefore, a technique to couple light via an active waveguiding process should be developed.

Here, we demonstrate that near-IR light can be coupled into organic nanofibre waveguides by utilising Raman scattering. As a sample, we used a nanofibre of thiacyanine (TC) dye (Fig. 1*a*) that propagates its fluorescence in the visible wavelength range (480–600 nm) by exciting it with a laser beam at $\lambda = 405$ nm. In this Letter, we illuminated the TC nanofibre with a focused laser beam at $\lambda = 785$ nm and observed that the Raman scattering with $\lambda = 800$–$910$ nm that was generated at the laser spot propagated along the nanofibre over its entire length of a few hundred micrometres. Propagation of Raman scattering along quasi-one-dimensional organic structures (tubular structures) was recently reported by Chandrasekhar *et al.* [16–18]. They mapped the spatial distribution of the Raman scattering over the tubes. In contrast, we measured the spectrum of light outcoupled from the fibre tip and quantitatively investigated the waveguiding properties of the TC nanofibre in the near-IR region.

**2. Experimental section**

2.1. Sample preparation: Approximately 0.2 mM TC solution was obtained by dissolving TC in hot water at ∼45°C. Then, the solution was cooled to room temperature, resulting in self-assembly of the TC molecules into single-crystalline nanofibres with lengths of up to ∼300 µm. The nanofibres had a rectangular cross section, and their width $d$ could be controlled from ∼20 nm to a few micrometres by varying the solution temperature and/or cooling speed [19]. A high solution temperature and rapid cooling result in the formation of narrower nanofibres. The samples were prepared by depositing the solution containing the nanofibres onto a glass substrate (microscope cover glass, 18 × 18 mm) and allowing the water to evaporate.

2.2. Optical measurements: An epi-illumination microscope (Olympus) equipped with a motorised stage (Prior) was used (Fig. 1*b*). The output of a continuous-wave diode laser ($\lambda = 785$ nm) was coupled to the microscope, directed toward the sample by a dichroic mirror (Semrock), and focused onto the sample with a 50 × IR objective lens (Olympus). The laser power at the sample was ∼10 mW. Scattered light from the sample was collected by the same objective lens and imaged onto the entrance slits of an imaging monochromator (Acton Research, SpectraPro 2150) through a long-pass filter (Semrock) that blocked the excitation laser. The light passing through the slits was recorded by a liquid-nitrogen-cooled back-illuminated charge-coupled device (CCD) camera (Princeton Instruments, Spec10, 1340 pixels × 400 pixels). The quantum efficiency of the CCD camera is ∼80% at $\lambda = 800$ nm and drops to ∼50% at $\lambda = 900$ nm. The captured image was spectrally and spatially resolved along the horizontal and vertical axes of the CCD camera, respectively.

To measure the waveguiding properties, a straight nanofibre was selected and positioned such that it was imaged between the entrance

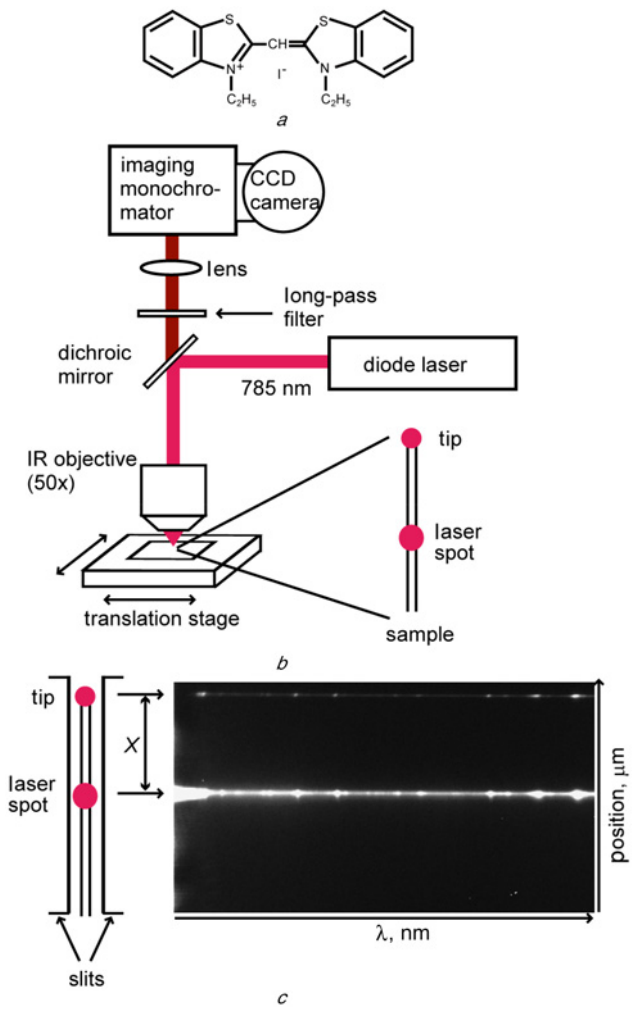


**Fig. 1** *Schematic representation of experimental setup*
*a* Chemical formula of TC
*b* Schematic of the experimental setup
*c* Left: a nanofibre imaged between the entrance slits of the monochromator (*X* is the distance between the laser spot and the nanofibre tip); right: an image captured by the CCD camera

slits of the monochromator by translating and rotating the sample (Fig. 1*c*). In this nanofibre orientation, the laser was polarised perpendicular to the fibre axis. Since the nanofibre was imaged between the entrance slits, the scattering from the position of the laser spot and outcoupled light from the fibre tip passed through the entrance slits and were recorded by the CCD camera. The spectra at both positions were obtained by extracting the horizontal cross sections of the image. The spectral and spatial resolutions were ~0.4 nm and ~1 μm, respectively. These spectra were measured while the excited position was moved along the nanofibre by translating the sample in a direction parallel to the slits, namely by changing the distance, *X*, between the laser spot and the nanofibre tip. The obtained set of spectra was then analysed to evaluate the propagation loss.

The setup used to measure the fluorescence guiding was essentially the same as that described above. A continuous-wave diode laser ($\lambda = 405$ nm), a set of a dichroic mirror and a long-pass filter (Omega optical), which were adequate for the excitation wavelength, and a 40× objective lens for visible light (Olympus) were used [20].

## 3. Results and discussion

3.1. Fluorescence guiding along a TC nanofibre: To clarify the difference in the waveguiding properties for visible light (fluorescence) and near-IR light (Raman scattering), first, we

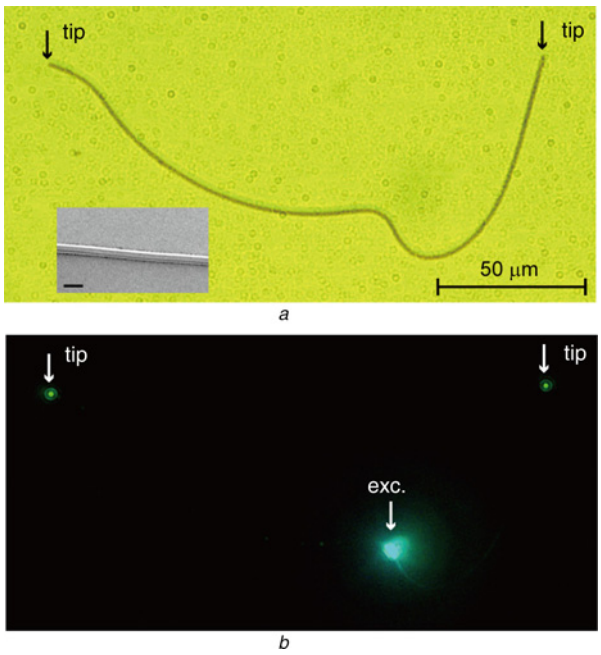


**Fig. 2** *Fluorescence guiding along a TC nanofibre*
*a* Optical micrograph of a TC nanofibre on a glass substrate (arrows indicate the tips of the fibre); inset: SEM image (scale bar is 1 μm)
*b* Fluorescence microscopy image of the nanofibre obtained by exciting the position indicated as Exc

briefly describe and discuss the fluorescence guiding properties of TC nanofibres, which we investigated in our previous studies [1, 20]. Fig. 2*a* shows an optical micrograph of a TC nanofibre with a length of ~250 μm and $d$ ; 400 nm that has been transferred onto a glass substrate. A scanning electron microscopy (SEM) image shows that the nanofibre has a very smooth surface (inset in Fig. 2*a*). When the point labelled "Exc." (position indicated in Fig. 2*b*) was illuminated with a focused 405 nm laser, which excites the exciton absorption band of the nanofibre, bright

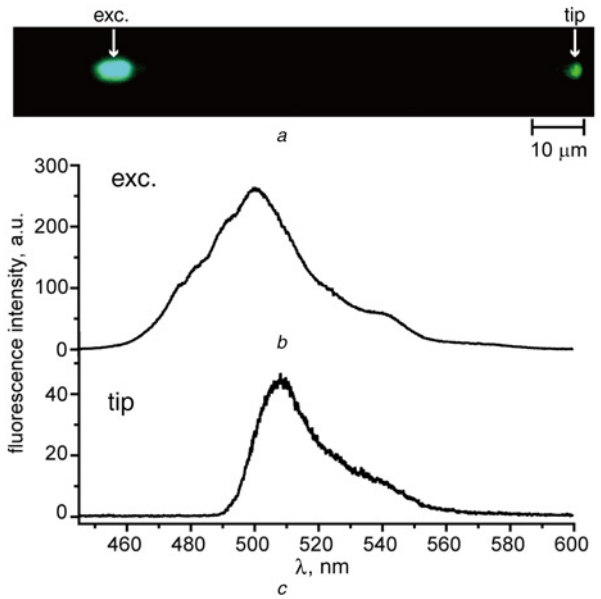


**Fig. 3** *Spatially resolved fluorescence spectra of a TC nanofibre*
*a* Fluorescence microscopy image of the straight nanofibre obtained by exciting the position labeled Exc
*b* Spatially resolved fluorescence spectrum at Exc
*c* Spatially resolved spectrum at the tip




doi: 10.1049/mnl.2016.0448

fluorescence spots were observed at both fibre tips, demonstrating the active fluorescence guiding behaviour (Fig. 2*b*).

Fig. 3*a* shows a fluorescence microscopy image of a straight TC nanofibre ($d$ ; 400 nm) recorded by exciting the point labelled Exc. The distance between that point and the tip ($X$) was 85.5 μm. By applying spatially resolved fluorescence microscopy as described in the Experimental section, the spectra at the excitation point and at the tip were obtained. The spectrum at the excitation point, which corresponds to the fluorescence spectrum of the nanofibre, shows fluorescence between 460 and 600 nm (Fig. 3*b*). In contrast, the spectrum at the tip shows fluorescence between 490 and 600 nm (Fig. 3*c*). These spectra indicate that fluorescence at $\lambda = 460$–490 nm is attenuated during propagation, whereas that at $\lambda = 490$–600 nm propagates to the tip.

By recording the spectra at the tip for various $X$ values, we can quantitatively determine the wavelength-dependent propagation loss via the procedure given in the next section. Our previous studies showed that for nanofibres with $d = 400$–800 nm, the loss at long wavelengths ($\lambda = 520$–600 nm) is small (<1 dB/100 μm) and increases with decreasing $\lambda$ [20]. Moreover, we applied spatially resolved fluorescence microscopy to bent nanofibres and observed that the fluorescence transmitted through sharply bent nanofibres with micron-scale radii of curvature suffered only small bending losses [5]. We revealed that the small bending losses can be attributed to the exciton polariton effect [21]. Namely, the guided fluorescence couples with excitons and forms exciton polaritons, which are strongly coupled states of photons and excitons [22, 23]. Polariton formation results in a substantially large high the refractive index of the nanofibres, which leads to small bending losses.

3.2. Raman scattering guiding along a TC nanofibre: To couple near-IR light into a TC nanofibre and investigate its waveguiding properties in this wavelength region, here we used Raman scattering instead of fluorescence emission. A nanofibre with $d$ ; 800 nm was illuminated with a focused laser beam at $\lambda = 785$ nm

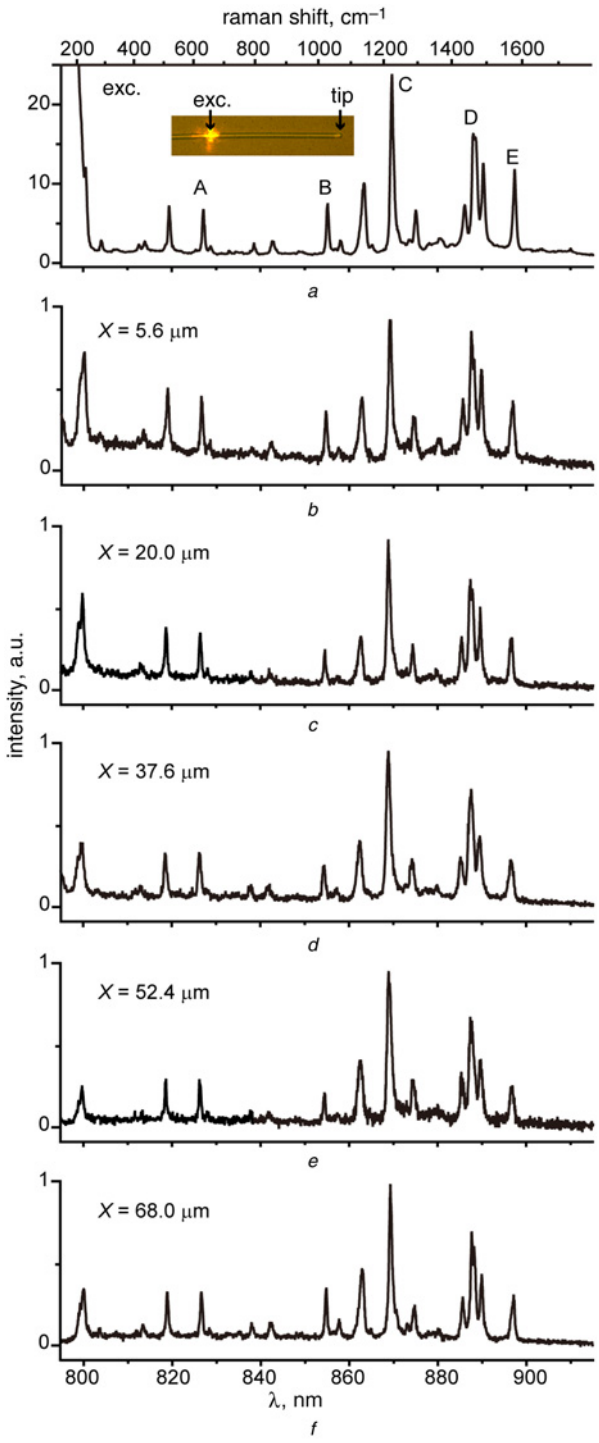


**Fig. 4** *Spatially resolved spectra of the nanofibre obtained by illuminating it with a laser beam at λ = 785 nm (see the inset of a)*
*a* Spectrum at the position of the laser spot, which corresponds to the Raman spectrum of the nanofibre
*b–f* Spectra measured at the nanofibre tip obtained by varying $X$ from 5.6 to 68.0 μm

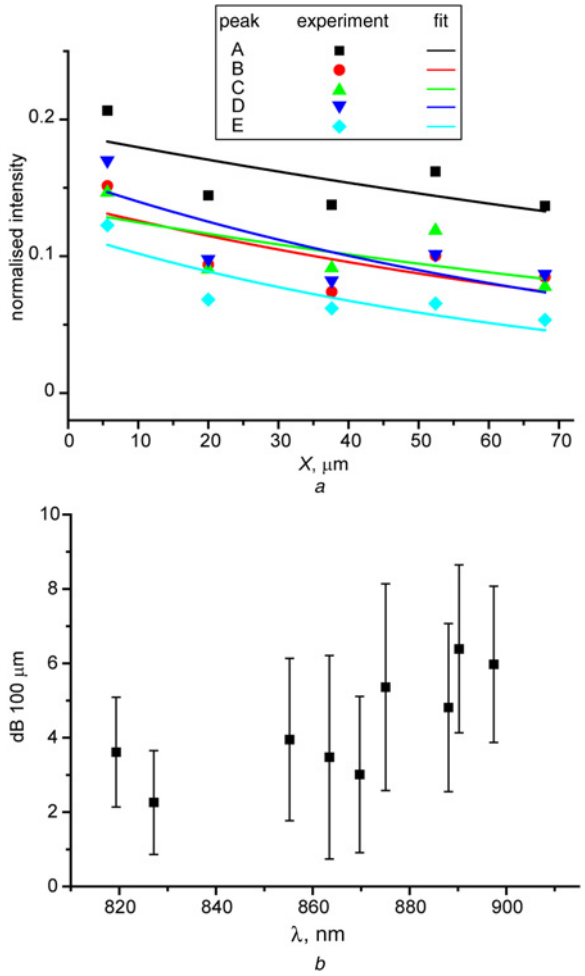


**Fig. 5**
*a* Normalised intensities of peaks A–E in Fig. 4*a* plotted as functions of $X$ (symbols) and best fitted curves
*b* Plot of the losses for $X = 100$ μm as a function of $\lambda$

(spot size: ~1 μm) (inset in Fig. 4*a*), and the spectra at the laser spot and the tip were recorded using spatially resolved microscopy. Fig. 4*a* shows the spectrum at the laser spot, which corresponds to the Raman spectrum of the nanofibre. Sharp Raman peaks were clearly observed in a wavelength range of 800–915 nm, which corresponds to a Raman shift of 200–1800 $cm^{-1}$ (see the top axis). The spectral range was limited to $\lambda < \sim 915$ nm by the sensitivity of the CCD camera. The features of the obtained Raman spectrum were similar to those of the spectra of other cyanines and TCs, both in solution and in their crystalline (aggregate) phase [24–26]. The Raman peaks observed in this wavenumber region were assigned to C–C stretching vibrations, CH out-of-plane bending vibrations, C = C stretching vibrations, and their coupled modes. The assignments of the individual Raman peaks in our spectrum are not given in this Letter because that is outside the scope of the present study.

Figs. 4*b–f* show the spectra at the tip of the nanofibre recorded while $X$ was varied from 5.6 to 68.0 μm. These spectra exhibit peaks at the same positions as the Raman peaks shown in Fig. 4*a*, indicating that the Raman scattering generated at the laser spot propagated to the tip and that near-IR light was coupled into the TC nanofibre.

We quantitatively analysed the propagation loss of the TC nanofibre for near-IR light as follows: First, the intensities of the peaks in the spectra at the tip (Figs. 4b–f) were normalised with respect to those of the corresponding peaks in the Raman spectra measured at the laser spot (Fig. 4*a*). Then, the normalised intensities were plotted as a function of $X$. As an example, the plots of several peaks (marked A–E in Fig. 4*a*) are shown in Fig. 5*a* (symbols). The data points show a gradual decrease with increasing $X$, which is attributed to the propagation loss. These data points were fitted by an exponential decay function expressed as $I(X) = I_0 \exp(-\alpha X)$, where $I_0$ is the normalisation coefficient, and $\alpha$ is a fitting parameter (solid curves). Using the obtained values of $\alpha$, the propagation loss across a distance $X$ can be evaluated using the equation $L(X) = -10 \log[I(X)/I_0]$ dB $= -10 \log[\exp(-\alpha X)]$ dB. We conducted this analysis for the nine major Raman peaks in the spectra and evaluated the losses for $X = 100$ μm [$L(100)$], which are plotted in Fig. 5*b* as a function of $\lambda$. For the short-wavelength side, $\lambda < 880$ nm, the nanofibre exhibited a relatively small propagation loss of ~4 dB/100 μm. This value is a few times larger than that for $\lambda = 500-600$ nm measured via fluorescence guiding [20]. The light–exciton coupling (the polariton effect) in the near-IR region should be weaker than that in the visible region because of the large energy difference between near-IR light and the exciton absorption band, which is located around $\lambda = 400$ nm [1]. The weak polariton effect leads to a small refractive index; thus, confinement of light in the nanofibre is weak. Therefore, the weak confinement, which results in more leakage of light from the nanofibre, can probably be attributed to the greater propagation loss in the near-IR region compared with that in the visible region. For the long-wavelength side, $\lambda = 880-900$ nm, the loss increased slightly to 5 −6 dB/100 μm. This supports the weakening of the confinement with increasing $\lambda$. To support the above discussion, we will numerically calculate the waveguiding properties in our future work.

The technique developed in this Letter has two major advantages. First, it can be applied to any nanofibre waveguide regardless of whether it is organic or inorganic, as long as it has Raman-active vibrational modes. Second, light with a wide wavelength range can be coupled into nanofibres by varying the wavelength of the excitation laser. In this Letter, we presented the results obtained using a 785 nm excitation laser. We also conducted the same experiment using a 632 nm laser (He–Ne laser) and observed that light with $\lambda >$ 650 nm could be coupled into the nanofibres. If suitable optical components and a detector are employed, it is possible to couple light with $\lambda > 1$ μm into nanofibres by using, for example a 1.06 μm laser. This will enable us to study the waveguiding properties of the nanofibres for the telecommunication wavelengths of 1.3 −1.5 μm. The waveguiding properties in this wavelength range are particularly important for examining the feasibility of telecommunication device applications of the nanofibres.

**4. Conclusion:** We developed a technique to couple near-IR light into organic nanofibre waveguides by utilising Raman scattering. As a sample, we used a nanofibre of TC, which propagates its fluorescence in the visible wavelength range (480–600 nm). We illuminated TC nanofibres with a laser beam at $\lambda = 785$ nm and observed that Raman scattering with $\lambda = 800–910$ nm generated at the laser spot propagated to the fibre tips over a distance of ~100 μm. We quantitatively investigated the waveguiding properties of the TC nanofibres for the near-IR range. The loss was ~4 dB/100 μm for $\lambda = 820–880$ nm and increased slightly with $\lambda$. Our next step is to apply this technique to bending loss measurement in the near-IR region because a low bending loss is essential for nanophotonics applications of nanofibres.

**5. Acknowledgment:** This Letter was supported by JSPS KAKENHI grant no. 15K04705.

## 6 References

[1] Takazawa K., Kitahama Y., Kimura Y., *ET AL.*: 'Optical waveguide self-assembled from organic dye molecules in solution', *Nano Lett.*, 2005, **5**, pp. 1293–1296
[2] Zhang C., Zhao Y.S., Yao J.N.: 'Optical waveguides at micro/nanoscale based on functional small organic molecules', *Phys. Chem. Chem. Phys.*, 2011, **13**, pp. 9060–9073
[3] Schiek M., Balzer F., Al-Shamery K., *ET AL.*: 'Organic molecular nanotechnology', *Small*, 2008, **4**, pp. 176–181
[4] Bao Q.L., Goh B.M., Yan B., *ET AL.*: 'Polarized emission and optical waveguide in crystalline perylene diimide microwires', *Adv. Mater.*, 2010, **22**, pp. 3661–3666
[5] Takazawa K.: 'Flexibility and bending loss of waveguiding molecular fibers self-assembled from thiacyanine dye', *Chem. Phys. Lett.*, 2008, **452**, pp. 168–172
[6] Takeda H., Sakoda K.: 'Bending losses of optically anisotropic exciton polaritons in organic molecular-crystal nanofibers', *Opt. Express*, 2013, **25**, pp. 31420–31429
[7] Takazawa K., Inoue J., Mitsuishi K., *ET AL.*: 'Micron-scale photonic circuit components based on propagation of exciton polaritons in organic dye nanofibers', *Adv. Mater.*, 2011, **23**, pp. 3659–3663
[8] Takazawa K., Inoue J., Mitsuishi K., *ET AL.*: 'Ultracompact asymmetric Mach-Zehnder interferometers with high visibility constructed from exciton polariton waveguides of organic dye nanofibers', *Adv. Funct. Mater.*, 2013, **23**, pp. 839–845
[9] Zhao Y.S., Peng A.D., Fu H.B., *ET AL.*: 'Nanowire waveguides and ultraviolet lasers based on small organic molecules', *Adv. Mater.*, 2008, **20**, pp. 1661–1665
[10] Zhang C., Zou C.L., Yan Y.L., *ET AL.*: 'Two-photon pumped lasing in single-crystal organic nanowire exciton polariton resonators', *J. Am. Chem. Soc.*, 2011, **133**, pp. 7276–7279
[11] Cui Q.H., Zhao Y.S., Yao J.N.: 'Photonic applications of one-dimensional organic single-crystalline nanostructures: optical waveguides and optically pumped lasers', *J. Mater. Chem.*, 2012, **22**, pp. 4136–4140
[12] Zhang C., Yan Y.L., Zhao Y.S., *ET AL.*: 'From molecular design and materials construction to organic nanophotonic devices', *Acc. Chem. Res.*, 2014, **47**, pp. 3448–3458
[13] Cui Q.H., Zhao Y.S., Yao J.N.: 'Controlled synthesis of organic nanophotonic materials with specific structures and compositions', *Adv. Mater.*, 2014, **26**, pp. 6852–6870
[14] Wei C., Liu S.Y., Zou C.L., *ET AL.*: 'Controlled self-assembly of organic composite microdisks for efficient output coupling of whispering-gallery-mode lasers', *J. Am. Chem. Soc.*, 2015, **137**, pp. 62–65
[15] Quochi F., Cordella F., Mura A., *ET AL.*: 'Gain amplification and lasing properties of individual organic nanofibers', *Appl. Phys. Lett.*, 2006, **88**, p. 041106
[16] Chandrasekhar N., Mohiddon M.A., Chandrasekar R.: 'Organic submicro tubular optical waveguides: self-assembly, diverse geometries, efficiency, and remote sensing properties', *Adv. Opt. Mater.*, 2013, **1**, pp. 305–311




doi: 10.1049/mnl.2016.0448

[17] Chandrasekar R.: 'Organic photonics: prospective nano/micro scale passive organic optical waveguides obtained from π-conjugated ligand molecules', *Phys. Chem. Chem. Phys.*, 2014, **16**, pp. 7173–7183
[18] Chandrasekhar N., Reddy E.R., Prasad M.D., *ET AL.*: 'Passive optical waveguiding tubular pharmaceutical solids and Raman spectroscopy/mapping of nano-/micro-scale defects', *Cryst. Eng. Comm.*, 2014, **16**, pp. 4696–4700
[19] Takazawa K., Inoue J., Mitsuishi K.: 'Optical waveguiding along a sub-100-nm-width organic nanofiber: significant effect of cooling on waveguiding properties', *J. Phys. Chem. C*, 2016, **120**, pp. 1186–1192
[20] Takazawa K.: 'Waveguiding properties of fiber-shaped aggregates self-assembled from thiacyanine dye molecules', *J. Phys. Chem. C*, 2007, **111**, pp. 8671–8676
[21] Takazawa K., Inoue J., Mitsuishi K., *ET AL.*: 'Fraction of a millimeter propagation of exciton polaritons in photoexcited nanofibers of organic dye', *Phys. Rev. Lett.*, 2010, **105**, p. 067401
[22] Takeda H., Sakoda K.: 'Exciton-polariton mediated light propagation in anisotropic waveguides', *Phys. Rev. B*, 2012, **86**, pp. 205319
[23] Hopfield J.J.: 'Theory of the contribution of excitons to the complex dielectric constant of crystals', *Phys. Rev.*, 1958, **112**, pp. 1555–1567
[24] Iwata K., Weaver W.L., Gustafson T.L.: 'Spontaneous Raman spectra of the cyanine dye DODCI and its six analogues using titanium:sapphire laser excitation', *J. Phys. Chem.*, 1992, **96**, pp. 10219–10224
[25] Li X.H., Gu B., Akins D.L.: 'Surface-enhanced Raman scattering by cyanine chloride', *Chem. Phys. Lett.*, 1984, **105**, pp. 263–267
[26] Akins D.L.: 'Resonance-enhanced Raman scattering by aggregated 2, 2′-cyanine on colloidal silver', *J. Colloid Interface Sci.*, 1982, **90**, pp. 373–379